




Article

Profiling of Widely Targeted Metabolomics for the Identification of Secondary Metabolites in Heartwood and Sapwood of the Red-Heart Chinese Fir (*Cunninghamia Lanceolata*)

Sen Cao ¹, Zijie Zhang ¹, Yuhan Sun ¹, Yun Li ^{1,*} and Huiquan Zheng ^{2,*}

¹ College of Biological Sciences and Technology, National Engineering Laboratory for Tree Breeding, Beijing Advanced Innovation Center for Tree Breeding by Molecular Design, Beijing Forestry University, Beijing 100083, China; caosen0419@bjfu.edu.cn (S.C.); zijiezhang@bjfu.edu.cn (Z.Z.); syh831008@163.com (Y.S.)

² Guangdong Provincial Key Laboratory of Silviculture, Protection and Utilization, Guangdong Academy of Forestry, Guangzhou 510520, China

* Correspondence: yunli@bjfu.edu.cn (Y.L.); zhenghq@sinogaf.cn (H.Z.); Tel./Fax: +86-10-6233-6094 (Y.L.)

Received: 20 July 2020; Accepted: 15 August 2020; Published: 18 August 2020



Abstract: The chemical composition of secondary metabolites is important for the quality control of wood products. In this study, the widely targeted metabolomics approach was used to analyze the metabolic profiles of heartwood and sapwood in the red-heart Chinese fir (*Cunninghamia lanceolata*), with an ultra-performance liquid chromatography-electrospray ionization tandem mass spectrometry system. A total of 224 secondary metabolites were detected in the heartwood and sapwood, and of these, flavonoids and phenolic acids accounted for 36% and 26% of the components, respectively. The main pathways appeared to be differentially activated, including those for the biosynthesis of phenylpropanoids and flavonoids. Moreover, we observed highly significant accumulation of naringenin chalcone, dihydrokaempferol, pinocembrin, hesperetin, and other important secondary metabolites in the flavonoid biosynthesis pathway. Our results provide insight into the flavonoid pathway associated with wood color formation in Chinese fir that will be useful for further breeding programs.

Keywords: Chinese fir; heartwood; secondary metabolites; widely targeted metabolomics; flavonoids

1. Introduction

The xylem of most woody plants can be divided into three parts: lighter sapwood (SW) on the periphery, darker heartwood (HW) on the inside, and the transition zone (TZ) at the color junction. HW contributes most to the value of the wood, and in most cases, it has a deep color that is likely associated with secondary metabolites. SW is often referred to as living tissue (5–25% of the components) and HW is mostly considered dead cells. The associated regulatory genes for metabolite production have been difficult to clarify in these tissues, particularly in HW. Some tree species have a TZ that produces secondary metabolites on a temporary basis, and includes live parenchyma cells; it is generally believed that this metabolic activity peaks rapidly in the TZ and produces a large number of secondary metabolites that accumulate in the HW [1].

Given the value of HW, some studies have specifically focused on its color. Miyamoto et al. [2] found that the moisture and potassium contents differed significantly between two groups of reddish and blackish HW in Sugi (*Cryptomeria japonica*). The color of HW in Scots pine (*Pinus sylvestris*) and Norway spruce (*Picea abies*) significantly changes after heat treatment, which may be due to

changes in the chemical properties of secondary metabolites [3]. Gierlinger et al. [4] concluded that the red hue (+a*) of Japanese larch (*Larix kaempferi*) HW was strongly correlated with the number of phenols ($r = 0.84$) and decay resistance ($r = 0.63$), suggesting that color measurements of larch HW could be valuable in tree breeding programs to create an optimized larch timber tree. In addition, Deklerck et al. [5] predicted the resistance of wood against fungal decay, and as such for wood quality by using DART-TOFMS, secondary metabolites, and Partial Least Squares. It is also worth noting that heritability of chemical composition is high, which implies that it may be possible to improve chemical composition through the genetic breeding of forest trees [6,7].

In plant species, color-related metabolites are referred to as polyphenols, and they include multiple phenolic groups that have strong antioxidant effects. Some studies have found that the color determination of wood flour is a good indicator of phenols. Higher phenol content and higher corrosion resistance can be achieved through breeding [6,7]. Flavonoids, which are polyphenols, mainly include anthocyanins, flavans, flavones, flavanones, flavonols, and chalcone and are also important components of plant secondary metabolites. They are synthesized from phenylalanine via the phenylpropanoid and flavonoid pathways in the cytoplasm, representing the most-studied pathways [8]. Flavonoids are widely found in colored fruits and flowers [9], and play important roles in a variety of plant functions, such as pigmentation, prevention of dormancy, fertility, prevention of damage by ultraviolet rays and plant pathogens, and prevention of biotic and abiotic stress [10]. They function as antioxidants that can prevent chronic diseases, including cardiovascular disease, certain types of cancer [11], and inflammation [12].

Widely targeted metabolomics based on multiple reaction monitoring (MRM) is a highly sensitive and accurate method to measure targeted metabolites and has the advantages of high throughput, high sensitivity, and wide coverage. This method has been commonly used to analyze metabolites in crop species, such as rice [13], black sesame [14], and *Chrysanthemum morifolium* [15], and has successfully identified many valuable metabolites. Widely targeted metabolomics has also been used to successfully identify some flavonoid compounds in crop species [16–18].

Chinese fir (*Cunninghamia lanceolata* (Lamb.) Hook.) is a fast-growing conifer tree species native to China that is well known as a quality wood used in the timber industry. This conifer has been used as a major breeding subject of the tree improvement programs of China for over 50 years [19], and numerous varieties were highlighted for their breeding value. Among them, the red-heart Chinese fir is particularly valuable because of its reddish HW [20]. Previous studies on red-heart Chinese fir have mainly focused on the collection and preservation of superior trees, the variation in the growth material based on provenance and family, the construction of seed orchards, and the breeding of seedlings [21–23]; few studies have investigated the mechanism underlying the color change in the wood. Fan et al. [24] found that contents of cold water, hot water, benzyl alcohol, ash, and 1% NaOH extracts in HW were higher than SW in the red-heart Chinese fir. Analyses of the chemical constituents of ethanol extracts of red-heart Chinese fir have demonstrated that two compounds, namely, cedrol and sclareol, are more concentrated in HW than in SW of the same age, and that the content increases with age [25]. In this context, we used a widely targeted metabolomics method to identify the main differences in metabolites between the HW and SW of the red-heart Chinese fir and described a metabolite base for further breeding programs.

2. Materials and Methods

2.1. Plant Materials

We used wood samples of 9-year-old red-heart Chinese fir belonging to clone cx746, collected from Xiaokeng State Forest Farm (Guangdong, China, 24°70' N, 113°81' E, 328–339 m above sea level). Three cores were collected from each individual tree from the main stems at breast height (1.3 m) using a tree growth cone and three random individuals were selected in clone cx746. The wood samples were split into two groups, based on color, and included SW in the outer wood, which was light yellow,

and HW in the inner wood with a deep red color. All samples were flash-frozen in liquid nitrogen and maintained at $-80\text{ }^{\circ}\text{C}$ for further use.

2.2. Extraction and Separation of Flavonoid Secondary Metabolites

The three red-heart Chinese fir wood core samples were mixed and freeze-dried under a vacuum, ground into a fine powder in liquid nitrogen, mixed thoroughly, and then crushed for 1.5 min at 30 Hz using a mixer mill (MM 400, Retsch) with zirconia beads. The samples (100 mg, per sample) were extracted with 1 mL 70% methanol on a rotating wheel at $4\text{ }^{\circ}\text{C}$ in the dark for 12 h. After centrifugation at 10,000 g for 10 min at $4\text{ }^{\circ}\text{C}$, the extracts were filtered (SCAA-104, $0.22\text{ }\mu\text{m}$ pore size; ANPEL) and then analyzed by LC-MS/MS (ThermoFisher Scientific, SanJose, CA, USA). Quality control samples were prepared by mixing all the samples equally. During the analyses, the quality control samples were run every 10 injections to monitor the stability of the analysis conditions.

The samples ($5\text{ }\mu\text{L}$, per sample) were analyzed using an ultra-performance liquid chromatography electrospray ionization tandem mass spectrometry (UPLC-ESI-MS/MS; hereafter, UEMS; SHIMADZU, Kyoto, Japan) system (Shim-pack UFLC SHIMADZU CBM30A, <http://www.shimadzu.com.cn/>; MS, Applied Biosystems 4500 QTRAP, <http://www.appliedbiosystems.com.cn/>) equipped with a C18 column (Waters ACQUITY UPLC HSS T3, $1.8\text{ }\mu\text{m}$, $2.1\text{ mm} \times 100\text{ mm}$). The mobile phases consisted of ultra-pure water containing 0.04 acetic acid as mobile phase A, and acetonitrile containing 0.04% acetic acid as mobile phase B. The A:B (*v/v*) gradient was as follows: 95:5 at 0 min, 5:95 at 11.0 min, 5:95 at 12.0 min, 95:5 at 12.1 min, and 95:5 at 15.0 min. The flow rate was maintained at 0.40 mL/min, and the column temperature was kept at $40\text{ }^{\circ}\text{C}$. All eluents were pure grades from Merck. The samples obtained above were also connected to an ESI-triple quadrupole-linear ion trap mass spectrometer (Applied Biosystems, Framingham, MA, USA) equipped with an atmospheric pressure chemical ionization (APCI) turbo-ion spray interface, operating in negative ion mode and controlled by Analyst 1.6.3 software (Sciex, Framingham, MA). The operating parameters of the APCI ion source were as follows: ESI temperature, $550\text{ }^{\circ}\text{C}$; Mass spec voltage, 5500 V; and curtain gas, 25 psi.

2.3. Metabolite Identification and Quantification

The identification and structural analyses of the primary and secondary spectral data of the metabolites detected by mass spectrometry were based on the MWDB database of Wuhan (China) Mettewell Biotechnology Co., Ltd (Wuhan, China). and public databases, including MassBank (<http://www.massbank.jp/>), KnapSack (<http://kanaya.naist.jp/KNAPsAcK/>) [26], HMDB (<http://www.hmdb.ca/>), MoToDB (<http://www.ab.wur.nl/moto/>), and METLIN (<http://metlin.scripps.edu/index.php>), and followed the standard metabolic operating procedures. Metabolomics data were processed using System Software Analyst (Version 1.6.3). Metabolite quantification was performed using MRM. Orthogonal partial least squares discriminant analysis (OPLS-DA) was performed on the identified metabolites. Metabolites with significant content differences were set as thresholds of variable importance in projection (VIP) ≥ 1 and fold change ≥ 2 or ≤ 0.5 .

2.4. Data Analyses

Principal component analysis (PCA) was employed to compress the original data into several principal components to describe the characteristics of the original data set [27]. The PC represents the combination of variables that explains most of the variance, in descending order. The main parameter obtained from PCA, R2X, represents the interpretation rate of the original data after dimensionality reduction and can be used to judge the quality of the model.

Partial least squares-discriminant analysis (PLS-DA) was used to help identify the differential metabolites. We also combined orthogonal signal correction (OSC) with PLS-DA being an OPLS-DA that further decomposes the X matrix into two types of information: related or unrelated to Y. OPLS-DA could filter differential variables by removing unrelated differences. The prediction parameters for evaluating the OPLS-DA model are R2X, R2Y, and Q2, where R2X and R2Y represent the interpretation

rate of the model built to the X and Y matrices, and Q2 represents the prediction ability of the model. The closer these three are to 1, the more stable the model. When $Q^2 > 0.5$, the model can be considered effective, and when $Q^2 > 0.9$, it can be considered excellent [28]. The OPLS-DA results enable a preliminary screening of differential metabolites between different tissues. In this study, a combination of the fold-change value and the VIP value was used to screen for differential metabolites. For the experiments, we used a completely randomized block design, and repeated the experiments three times. Microsoft Excel 2016 (Microsoft, Seattle, WA, USA) and IBM SPSS Statistics 24.0 (IBM Corporation, Armonk, NY, USA) were also used to evaluate the data assessed differential secondary metabolites. Differences in metabolites in HW and SW were evaluated using analysis of variance (ANOVA) with Duncan's multiple range tests for multiple comparisons. A p -value ≤ 0.05 for the ANOVA F-test was considered statistically significant.

3. Results

3.1. Metabolic Profiling of Heartwood and Sapwood Based on LC-MS/MS

To investigate differences in the composition of secondary metabolites between the HW and SW of the red-heart Chinese fir, widely targeted metabolomics assay was performed, which analyzed the metabolic spectrum using UEMS. Metabolites were quantitatively analyzed following the collection of secondary data using the MRM model. Collectively, a total of 224 secondary metabolites were covered in our assay (HW and SW; Figure 1A), including 80 flavonoids, 58 phenolic acids, 14 alkaloids, 9 lignans and coumarins, 7 tannins, 4 terpenoids, and 52 others (Figure 1B). Among these secondary metabolites, the most abundant were flavonoids.

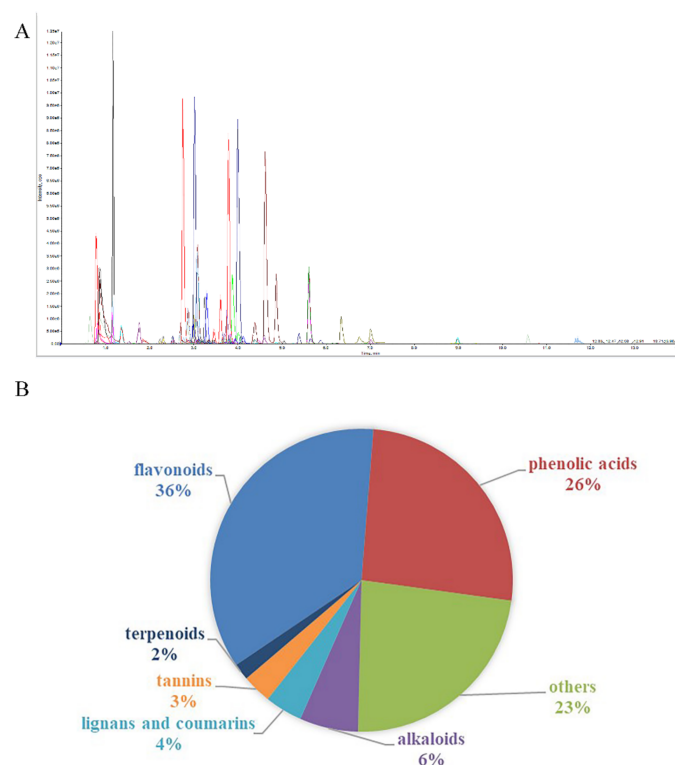


Figure 1. (A) The extracting ion current (XIC) chromatogram for the heart- and sapwood mix samples in a preliminary assay. (B) Types and proportions of differential secondary metabolites between heartwood and sapwood in the red-heart Chinese fir.

3.2. PCA

To compare the secondary metabolites in the HW and SW, the dataset obtained from the LC-MS/MS in ESI⁺ mode was subjected to PCA. In the PC1 × PC2 value plot (Figure 2B), the samples were separated in the first principal component (PC1), which reached 60.01%. The model of PC1 and PC2 explained 79.04% of the variance in total and showed different metabolites between the heartwood and sapwood. The results showed a distinct grouping of HW and SW samples into two distinct areas in the plot, indicating that each cultivar had a relatively distinct metabolic profile. In addition, multivariate statistics were used to assess further the differences in metabolic profiles between HW and SW, and hierarchical cluster analysis (HCA) of the secondary metabolites in HW and SW was also performed. This showed two main clusters based on the relative differences in the accumulation patterns in the different tissues (Figure 2C). The secondary metabolites belonging to cluster 1 accumulated at higher levels in SW and in contrast, the metabolites in cluster 2 accumulated at higher levels in HW. Taken together, the plot shows that there were significant differences in the secondary metabolites detected in HW and SW.

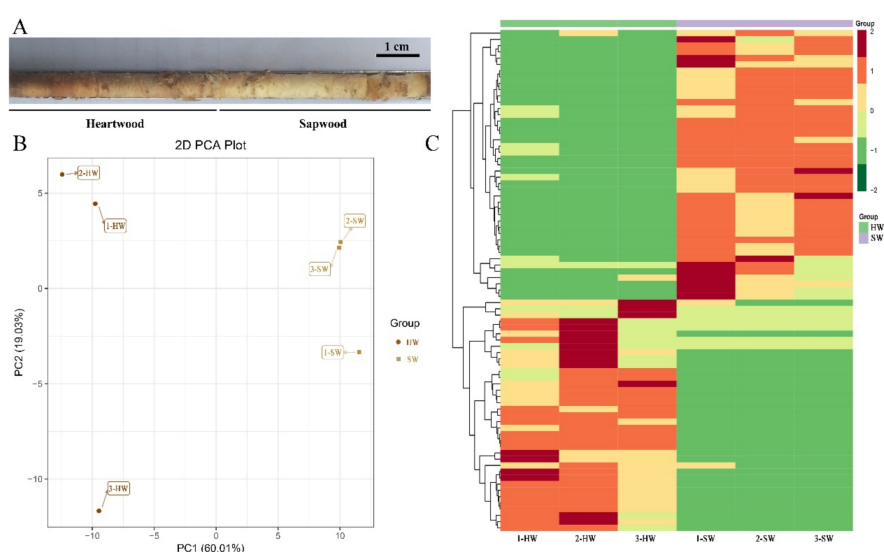


Figure 2. (A) A core of red-heart Chinese fir wood, showing red-colored tissue (heartwood, HW) and light-yellow tissue (sapwood, SW). (B) PCA score plot of the metabolites in the heartwood and sapwood. (C) Heatmap of the metabolites in the heartwood and sapwood.

3.3. OPLS-DA

The OPLS-DA model was used to screen the differential compounds in both groups of samples and analyze metabolic differences between HW and SW (Figure 3B). We observed high predictability (Q^2) and strong goodness of fit (R^2X , R^2Y) between HW and SW ($Q^2Y = 0.998$, $R^2X = 0.898$, $R^2Y = 1.000$). The HW was separated from SW, indicating major differences in the metabolic profiles between the two different colored tissues. Moreover, fold-change scores of ≥ 2 or ≤ 0.5 among the metabolites with a VIP value ≥ 1 was used to identify different metabolites. The screening results were analyzed using volcano plots (Figure 3A). A total of 80 significant differences between metabolites were identified, of which 37 were significantly up-regulated (the relative content of heartwood is larger than that of sapwood) and 43 were significantly down-regulated in HW and SW, respectively. The top 10 metabolites that were significantly up-regulated in HW are listed in Table 1, and among them, 6 flavonoids and 2 phenolic acids were significantly different between the HW and SW. These metabolites were mainly flavonoids and they can be considered the representative differential metabolites of HW and SW, influencing the properties and particularly the color of the wood.

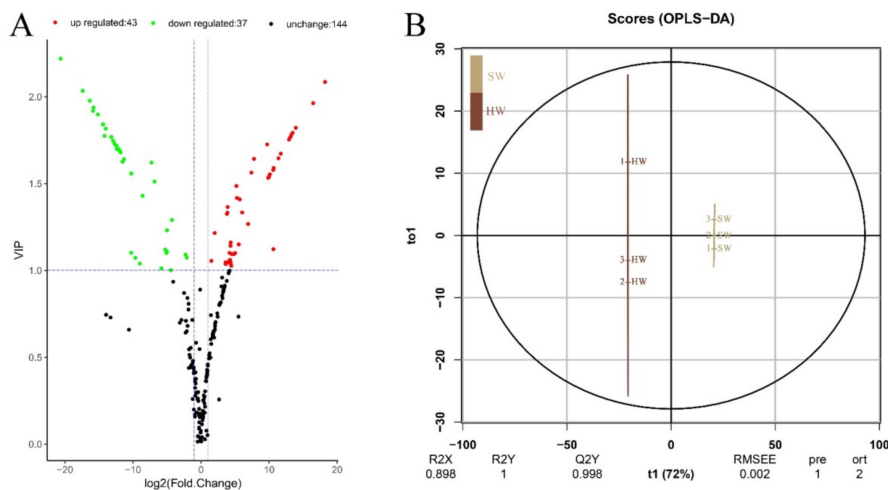


Figure 3. (A) The volcano plot of the differential metabolites in the heartwood and sapwood. Green dots represent down-regulated metabolites, red spots represent up-regulated metabolites, and gray dots represent insignificant differences in metabolites. (B) OPLS-DA model plot of the differential metabolites in the heartwood and sapwood.

Table 1. The top 10 metabolites that were significantly up-regulated in heartwood compared to sapwood.

Compounds	Formula	Class	VIP	Fold-Change	Log ² FC
Naringenin chalcone	C ₁₅ H ₁₂ O ₅	Flavonoids	2.22	1.65 × 10 ⁶	20.65
Dihydrokaempferol	C ₁₅ H ₁₂ O ₆	Flavonoids	2.03	1.73 × 10 ⁵	17.40
1-Feruloyl-sn-glycerol	C ₁₃ H ₁₆ O ₆	Phenolic acids	1.98	8.43 × 10 ⁴	16.36
Ailantinol E	C ₂₁ H ₂₄ O ₇	Others	1.92	6.04 × 10 ⁴	15.88
Pinocembrin (Dihydrochrysin)	C ₁₅ H ₁₂ O ₄	Flavonoids	1.94	5.66 × 10 ⁴	15.79
Z-6,7-Epoxyiligustilide	C ₁₂ H ₁₄ O ₃	Others	1.90	3.69 × 10 ⁴	15.17
3-O-Acetylpinobanksin	C ₁₇ H ₁₄ O ₆	Flavonoids	1.84	2.20 × 10 ⁴	14.43
benzoyltartaric acid	C ₁₁ H ₁₀ O ₇	Phenolic acids	1.84	2.12 × 10 ⁴	14.37
Sexangularetin	C ₁₆ H ₁₂ O ₇	Flavonoids	1.77	1.85 × 10 ⁴	14.18
Quercetin galloglucoside	C ₂₈ H ₂₄ O ₁₆	Flavonoids	1.82	1.66 × 10 ⁴	14.02

3.4. Putative Metabolic Pathways for Signal Metabolites

To elucidate the pathways of the differential metabolites, we mapped the metabolites from the HW and SW to the Kyoto Encyclopedia of Genes and Genomes (KEGG) database (<http://www.genome.jp/kegg/>). The results are shown in Figure 4A. These differential metabolites are mainly involved in metabolic pathways and flavonoid biosynthesis, and others, such as phenylpropanoids, flavone, and flavonol also showed differences. Flavonoids synthesized via the general phenylpropanoid pathway constitute a group of secondary metabolites in plants that contribute to the key characteristics of HW in woody plants, such as decay resistance and insect decay [29,30]. Further enrichment analyses of the main secondary metabolites showed that they were highly enriched in the flavonoid synthesis pathway, as shown in Figure 4B, and that flavonoids constituted the main secondary metabolite difference between HW and SW. Cellulose, hemicellulose, and lignin, which are the major components of wood, generally do not exhibit color; wood color is due to the presence of colored extractives contained in the wood. These colored extractives turn from pale to dark due to oxidation and polymerization over time.

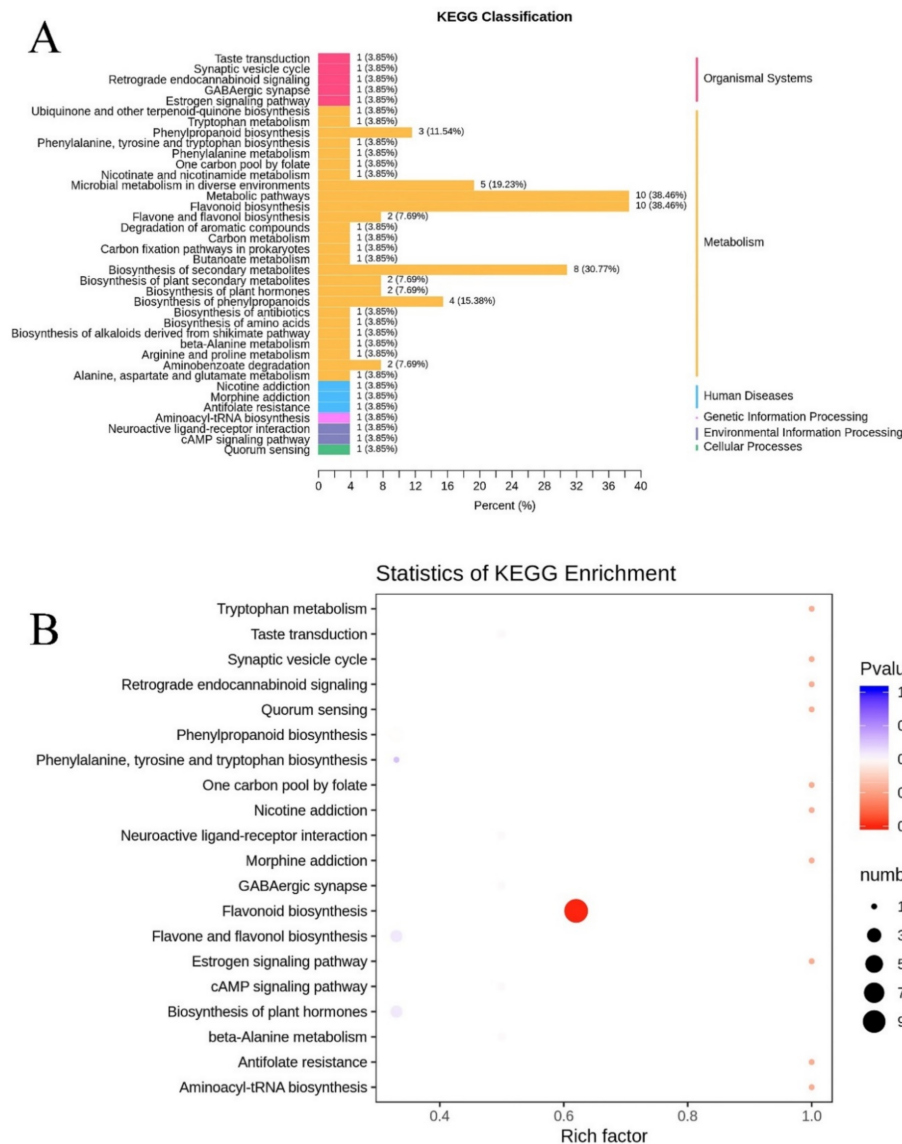


Figure 4. (A) Enrichment of the differential metabolites to highlight the KEGG pathway. Differential metabolites in the heartwood compared to those in the sapwood were mapped to distinct metabolic pathways. (B) Overview of pathway analyses of the heartwood and sapwood of the red-heart Chinese fir. The flavonoid biosynthesis metabolites are the most significantly different.

3.5. Secondary Metabolites Identified in the Flavonoid Pathway in HW and SW

Eleven significantly different secondary metabolites in the HW and SW of red-heart Chinese fir were selected for further analyses of the flavonoid pathway, and the differences are shown in Figure 5. The contents of naringenin chalcone, dihydrokaempferol, pinocembrin, hesperetin, pinobanksin, eriodictyol, luteolin, catechin, and apigenin were significantly higher in the HW than in SW, while the contents of epicatchin and myricetin were significantly higher in the SW than in HW. The annotation of the differential secondary metabolites to the flavonoid pathway, as shown in Figure 6, revealed that the Log_2FC values of naringenin chalcone, dihydrokaempferol, pinocembrin, and hesperetin were higher than 10 and were mainly concentrated in the upstream pathway. Myricetin, a downstream compound of dihydromyricetin, was more prevalent in SW than in HW, with a Log_2FC value of 10.6.

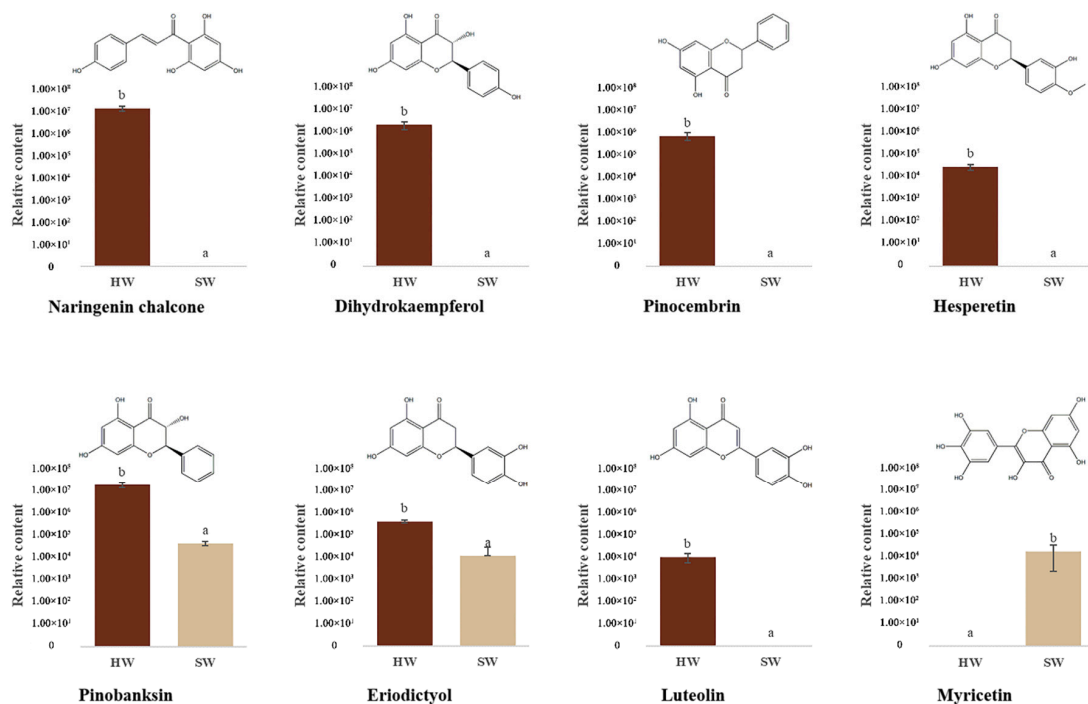


Figure 5. Chemical structure and contents of 8 significant differential flavonoids metabolites in the heartwood and sapwood of the red-heart Chinese fir. Means with different lowercase letters are significantly different at $p \leq 0.05$.

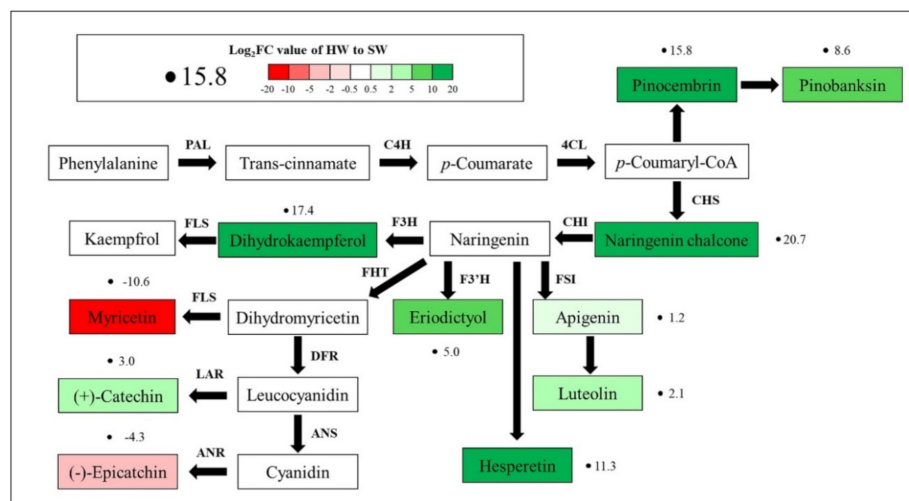


Figure 6. Metabolic profiling of the heartwood and sapwood in the flavonoid biosynthetic pathways in the red-heart Chinese fir. Grids with green and red color-scales from light to dark represent the Log_2FC values of HW to SW 0.5–2, 2–5, 5–10, 10–20, and over 20, respectively. PAL, phenylalanine ammonia-lyase; C4H, cinnamic acid 4-hydroxylase; 4CL, 4-coumarate CoA ligase; CHS, chalcone synthase; CHI, chalcone isomerase; F3H, flavanone 3-hydroxylase; F3'H, flavanoid 3'-hydroxylase; FHT, flavanone hydroxylase; FSI, flavonol synthase; DFR, dihydroflavonol 4-reductase; ANS, anthocyanidin synthase; FLS, flavonol synthesis; LAR, leucocyanidin reductase; ANR, anthocyanin reductase.

4. Discussion

We compared the secondary metabolites of the HW and SW in the red-heart Chinese fir by widely targeted metabolomics analyses, based on the UEMS system. There was a significant difference in the presence of 80 secondary metabolites. Metabolic pathway analyses revealed that the flavonoid

biosynthesis pathway was significantly different between HW and SW. Furthermore, HW contained significantly more flavonoids than SW.

There are considerably more metabolites in the plant kingdom than in the animal kingdom, with the number estimated to exceed 200,000 [31]. New varieties of woody plants are deliberately selected for the creation of high-quality wood. However, differences have only recently been discovered in the distribution of secondary metabolites in the stems of the red-heart Chinese fir. A metabolomics study can provide new information on the different secondary metabolic compound profiles. Detailed metabolite profiling of thousands of plant samples has great potential to elucidate metabolic processes. However, it is difficult to simultaneously undertake both comprehensive and high-throughput analyses in plants due to the wide diversity of metabolites present. Widely targeted metabolomics approach can monitor both the specific precursor ions and the product ions of each metabolite using MRM and tandem quadrupole mass spectrometry (TQMS), as they enable high sensitivity, reproducibility, and a broad dynamic range [32]. In general, such analyses can provide a large data set that will aid understanding of plant metabolism, and which can be used in combination with other omics approaches to achieve a deeper understanding of the biological processes involved. Herein, the UEMS system-based widely targeted metabolomics analyses approach appeared to be effective as it helps us to rapidly obtain information on 80 significantly different metabolites between HW and SW and to classify them accurately in Chinese fir.

Color differences are widely studied in horticulture and agriculture, and particularly in plants that are usually propagated vegetatively, such as most fruit trees. Cho et al. [33] analyzed the metabolites of three colored potato cultivars and found differences in the anthocyanin content. Xue et al. [34] analyzed the molecular and metabolic bases of pigmentation in *Lonicera japonica* flowers at different developmental stages and constructed regulatory networks of anthocyanin biosynthesis, chlorophyll metabolism, and carotenoid biosynthesis by weighted gene co-expression network analysis. In addition, there have been color-related studies on fig (*Ficus carica* L.), loquat (*Eriobotrya japonica* Lindl), pomegranate (*Punica granatum* L.), and other fruit trees [35–39]. Anthocyanins and flavonoids affect the colors and tastes of fruits; their antioxidant capacities confer health properties and reduce the risk for cardiovascular morbidity and mortality [40,41]. As with many secondary metabolite pathways, the flavonoid pathway is regulated by multiple genes. First, phenylalanine ammonia-lyase (PAL) catalyzes the conversion of phenylalanine into cinnamic acid. Then, dihydrokaempferol is converted from cinnamic acid by a series of enzymes, such as cinnamate 4 hydroxylase (C4H), 4-coumaroyl: CoA-ligase (4CL), chalcone synthase (CHS), chalcone isomerase (CHI), flavanone 3-hydroxylase (F3H), flavanone 3'-hydroxylase (F3'H), and flavanone 3'-5'-hydroxylase (F3'5'H). Subsequently, dihydroflavonol 4-reductase (DFR) catalyzes the conversion of dihydrokaempferol into unmodified and colorless anthocyanins [42,43]. Then, the conversion of colorless anthocyanins into colored anthocyanins is catalyzed by anthocyanidin synthase (ANS). Finally, the unstable colored anthocyanins are converted into blue-purple, brick red, or magenta glycosides by UDP glucose: flavonoid 3-O glucosyltransferase (UGT) [44–46]. In this study, we identified the flavonoids in the HW of the red-heart Chinese fir, determined which substances differed from those in the SW, and more importantly, revealed the highly significant accumulation of naringenin chalcone, dihydrokaempferol, pinocembrin, hesperetin, and other important secondary metabolites in the flavonoid biosynthesis pathway. We found that flavonoids were the secondary metabolites that differed most between the SW and HW in the red-heart Chinese fir. In addition, HW with a natural red-orange color differed from SW due to the presence of pigments that proved difficult to extract but which were formed by the enzymatic reduction of dihydroquercetin, the main extractive of Douglas fir HW [47,48]. Pâques et al. [49] found that taxifolin and dihydrokaempferol showed significant differences among different varieties of larch by studying the distribution of HW extractives in hybrid larches and in their related European and Japanese larch parents. Takahashi and Mori [50] concluded that Sugi HW turns black because sequirin-C, a type of norlignan that is readily soluble in alkaline solution and can form a large intramolecular conjugation system when alkalinized, was converted into products that had a deep purple color as the HW was basified. In another study, the metabolic

profiles of HW and SW in *Taxus chinensis* were analyzed using widely targeted metabolomics assay, and a total of 607 metabolites were detected, including 71 flavonoids and isoflavones that were significantly different between HW and SW [51]. The differences in the secondary metabolites of HW are mainly a result of species differences. This is due to the great diversity of metabolic pathways that each plant species has evolved to survive under varying environmental conditions.

In our study, flavonoids were the main secondary metabolites that differed between the HW and SW in the red-heart Chinese fir, but it is not known if they underlie the differences in color, as this requires additional evidence. Anthocyanins, as downstream products in the flavonoid biosynthesis pathway, are widely distributed in flowers and fruits, where they play a role in coloring, but there are few reports of anthocyanins in wood. In the transition zone, the ray parenchyma cells synthesize flavonoids before programmed death and eventually become a part of the heartwood [52,53]. This process increases the wood quality and corrosion resistance, while giving the heartwood a more attractive color. In future studies, we will compare the secondary metabolites of HW between the red-heart Chinese fir and the common Chinese fir at a population scale, in the hope that it will address this issue more intuitively. In addition, metabolomics, in combination with genomics, transcriptomics, or proteomics, may help us to analyze molecules with similar chemical properties that are related to metabolites (namely, DNA, RNA, and proteins).

5. Conclusions

This study was the first to investigate the differential secondary metabolites of the red-heart Chinese fir using a widely targeted metabolomics method. We found significant differences between HW and SW. This study successfully identified components in the HW of the red-heart Chinese fir that are consistent with specific characteristics of HW in other conifers. The results provide critical metabolite inventory information for the study of specific metabolites in the HW of the red-heart Chinese fir, and provide a base study for the improvement of wood quality regarding to HW color on the metabolite aspect.

Author Contributions: Y.L. and H.Z. conceived and designed the experiments, S.C. wrote the paper, S.C. and Z.Z. performed the experiments and analyzed the data, Y.S. participated in and help to complete the experiments. All authors have read and agreed to the published version of the manuscript.

Funding: This research was supported by the Key-Area Research and Development Program of Guangdong Province (No. 2020B020215001), the Science and Technology Research Project of Beijing Forestry University (No. 2018WS01) and the National Natural Science Foundation of China (No. 31972956).

Conflicts of Interest: The authors declare no conflict of interest.

References

1. Spicer, R. Senescence in secondary xylem: Heartwood formation as an active developmental program. In *Vascular Transport in Plants*; Elsevier: Amsterdam, The Netherland, 2005; pp. 457–475.
2. Miyamoto, N.; Iizuka, K.; Nasu, J.; Yamada, H. Genetic effects on heartwood color variation in *Cryptomeria japonica*. *Silvae Genet.* **2016**, *65*, 80–87. [[CrossRef](#)]
3. Sundqvist, B. Color response of Scots pine (*Pinus sylvestris*), Norway spruce (*Picea abies*) and birch (*Betula pubescens*) subjected to heat treatment in capillary phase. *Eur. J. Wood Wood Prod.* **2002**, *60*, 106–114. [[CrossRef](#)]
4. Gierlinger, N.; Jacques, D.; Grabner, M.; Wimmer, R.; Schwanninger, M.; Rozenberg, P.; Pâques, L.E. Colour of larch heartwood and relationships to extractives and brown-rot decay resistance. *Trees-Struct. Funct.* **2004**, *18*, 102–108. [[CrossRef](#)]
5. Deklerck, V.; De Ligne, L.; Espinoza, E.; Beeckman, H.; Van den Bulcke, J.; Van Acker, J. Assessing the natural durability of xylarium specimens: Mini-block testing and chemical fingerprinting for small-sized samples. *Wood Sci. Technol.* **2020**, *54*, 981–1000. [[CrossRef](#)]
6. Fries, A.; Ericsson, T.; Gref, R. High heritability of wood extractives in *Pinus sylvestris* progeny tests. *Can. J. For. Res.* **2000**, *30*, 1707–1713. [[CrossRef](#)]

7. Ericsson, T.; Fries, A.; Gref, R. Genetic correlations of heartwood extractives in *Pinus sylvestris* progeny tests. *For. Genet.* **2001**, *8*, 73–80.
8. Jeong, S.T.; Goto-Yamamoto, N.; Kobayashi, S.; Esaka, M. Effects of plant hormones and shading on the accumulation of anthocyanins and the expression of anthocyanin biosynthetic genes in grape berry skins. *Plant Sci.* **2004**, *167*, 247–252. [[CrossRef](#)]
9. Gould, K.; Davies, K.M.; Winefield, C. *Anthocyanins: Biosynthesis, Functions, and Applications*; Springer Science & Business Media: Berlin/Heidelberg, Germany, 2008.
10. Jia, L.; Wu, Q.; Ye, N.; Liu, R.; Shi, L.; Xu, W.; Zhi, H.; Rahman, A.R.B.; Xia, Y.; Zhang, J. Proanthocyanidins inhibit seed germination by maintaining a high level of abscisic acid in *Arabidopsis thaliana* F. *J. Integr. Plant Biol.* **2012**, *54*, 663–673. [[CrossRef](#)]
11. Sehitoglu, M.H.; Farooqi, A.A.; Qureshi, M.Z.; Butt, G.; Aras, A. Anthocyanins: Targeting of signaling networks in cancer cells. *Asian Pac. J. Cancer Prev.* **2014**, *15*, 2379–2381. [[CrossRef](#)]
12. Lee, S.L.; Chin, T.Y.; Tu, S.C.; Wang, Y.J.; Hsu, Y.T.; Kao, M.C.; Wu, Y.C. Purple sweet potato leaf extract induces apoptosis and reduces inflammatory adipokine expression in 3T3-L1 differentiated adipocytes. *Evid. Based Complement. Altern. Med.* **2015**, 126302. [[CrossRef](#)]
13. Wei, C.; Liang, G.; Guo, Z.; Wang, W.; Zhang, H.; Liu, X.; Yu, S. A novel integrated method for large-scale detection, identification, and quantification of widely targeted metabolites: Application in the study of rice metabolomics. *Mol. Plant* **2013**, *6*, 1769–1780. [[CrossRef](#)]
14. Wang, D.; Zhang, L.; Huang, X.; Xiao, W.; Yang, R.; Jin, M.; Wang, X.; Wang, X.; Qi, Z.; Li, P. Identification of nutritional components in black sesame determined by widely targeted metabolomics and traditional Chinese Medicines. *Molecules* **2018**, *23*, 1180. [[CrossRef](#)]
15. Wang, T.; Zou, Q.; Guo, Q.; Yang, F.; Zhang, W. Widely targeted metabolomics analysis reveals the effect of flooding stress on the synthesis of flavonoids in *Chrysanthemum morifolium*. *Molecules* **2019**, *24*, 3695. [[CrossRef](#)]
16. Wu, X.; Prior, R.L. Systematic identification and characterization of anthocyanins by HPLC-ESI-MS/MS in common foods in the United States: Fruits and Berries. *J. Agric. Food Chem.* **2005**, *53*, 2589–2599. [[CrossRef](#)]
17. Lin, L.Z.; Sun, J.; Chen, P.; Harnly, J.A. LC-PDA-ESI/MS(n) Identification of New Anthocyanins in purple bordeaux radish (*Raphanus sativus* L. variety). *J. Agric. Food Chem.* **2011**, *59*, 6616–6627. [[CrossRef](#)]
18. Sun, J.; Lin, L.Z.; Pei, C. Study of the mass spectrometric behaviors of anthocyanins in negative ionization mode and its applications for characterization of anthocyanins and non-anthocyanin polyphenols. *Rapid Commun. Mass Spectrom.* **2012**, *26*, 1123–1133. [[CrossRef](#)]
19. Zheng, H.; Hu, D.; Wei, R.; Yan, S.; Wang, R. Chinese fir breeding in the high-throughput sequencing era: Insights from SNPs. *Forests* **2019**, *10*, 681. [[CrossRef](#)]
20. Duan, H.; Hu, R.; Wu, B.; Chen, D.; Huang, K.; Dai, J.; Chen, Q.; Wei, Z.; Cao, S.; Sun, Y. Genetic characterization of red-colored heartwood genotypes of Chinese fir using simple sequence repeat (SSR) markers. *Genet. Mol. Res.* **2015**, *14*, 18552–18561. [[CrossRef](#)]
21. Qiu, F.; Sun, S.; Xiao, F.; Zeng, Z.; Liang, C.; Liang, X. Growth analysis of half-sib families from first generation seed orchard of *Cunninghamia lanceolata*. *South China For. Sci.* **2016**, *44*, 1–4. (In Chinese) [[CrossRef](#)]
22. Kui-Peng, L.I.; Wei, Z.C.; Huang, K.Y.; Dong, L.J.; Huang, H.F.; Chen, Q.; Dai, J.; Tan, W.J. Research on variation pattern of wood properties of red-heart Chinese fir plus trees, a featured provenance from Rongshui of Guangxi. *For. Res.* **2017**, *30*, 424–429. (In Chinese) [[CrossRef](#)]
23. Wen, H.; Deng, X.; Zhang, Y.; Wei, X.; Zhu, N. *Cunninghamia lanceolata* variant with red-heart wood: A mini-review. *Dendrobiology* **2018**, *79*, 156–167. [[CrossRef](#)]
24. Fan, G.R.; Zhang, W.Y.; Xiao, F.M.; Zhu, X.Z.; Jiang, X.M.; Yan-Shan, L.I. Studies on longitudinal variation of main chemical components in Chenshan red-heart Chinese-fir. *Acta Agric. Univ. Jiangxiensis* **2015**, *37*, 212–217. (In Chinese) [[CrossRef](#)]
25. Yang, H.; Wen, S.; Xiao, F.; Fan, G. Study on the chemical compositions of ethanol extraction from Chenshan Red-heart Chinese fir. *South China For. Sci.* **2016**, *44*, 35–37. (In Chinese) [[CrossRef](#)]
26. Afendi, F.M.; Okada, T.; Yamazaki, M.; Hirai-Morita, A.; Nakamura, Y.; Nakamura, K.; Ikeda, S.; Takahashi, H.; Altaf-Ul-Amin, M.; Darusman, L.K.; et al. KNApSACk family databases: Integrated metabolite-plant species databases for multifaceted plant research. *Plant Cell Physiol.* **2012**, *53*, e1. [[CrossRef](#)]
27. Eriksson, L.; Kettanehwoold, N.; Trygg, J.; Wikström, C.; Wold, S. Part I: Basic Principles and Applications. In *Multi- and Megavariate Data Analysis*, 2nd ed.; Umetrics Academy: Umea, Sweden, 2006.

28. Thevenot, E.A.; Roux, A.; Xu, Y.; Ezan, E.; Junot, C. Analysis of the human adult urinary metabolome variations with age, body mass index, and gender by implementing a comprehensive workflow for univariate and opls statistical analyses. *J. Proteome Res.* **2015**, *14*, 3322–3335. [[CrossRef](#)]
29. Mounquengui, S.; Tchinda, J.B.S.; Ndikontar, M.K.; Dumarçay, S.; Attéké, C.; Perrin, D.; Gelhaye, E.; Gérardin, P. Total phenolic and lignin contents, phytochemical screening, antioxidant and fungal inhibition properties of the heartwood extractives of ten Congo Basin tree species. *Ann. For. Sci.* **2016**, *73*, 287–296. [[CrossRef](#)]
30. Gierlinger, N.; Jacques, D.; Schwanninger, M.; Wimmer, R.; Pâques, L.E. Heartwood extractives and lignin content of different larch species (*Larix* sp.) and relationships to brown-rot decay-resistance. *Trees* **2004**, *18*, 230–236. [[CrossRef](#)]
31. Fiehn, O.; Kloska, S.; Altmann, T. Integrated studies on plant biology using multiparallel techniques. *Curr. Opin. Biotechnol.* **2001**, *12*, 82–86. [[CrossRef](#)]
32. Sawada, Y. Widely targeted metabolomics based on large-scale MS/MS Data for elucidating metabolite accumulation patterns in plants. *Plant Cell Physiol.* **2009**, *50*, 37–47. [[CrossRef](#)]
33. Cho, K.; Cho, K.; Sohn, H.; Ha, I.J.; Hong, S.; Lee, H.; Kim, Y.; Nam, M.H. Network analysis of the metabolome and transcriptome reveals novel regulation of potato pigmentation. *J. Exp. Bot.* **2016**, *67*, 1519–1533. [[CrossRef](#)]
34. Xue, Q.; Fan, H.; Yao, F.; Cao, X.; Liu, M.; Sun, J.; Liu, Y. Transcriptomics and targeted metabolomics profilings for elucidation of pigmentation in *Lonicera japonica* flowers at different developmental stages. *Ind. Crop. Prod.* **2020**, *145*, 111981. [[CrossRef](#)]
35. Hadjipieri, M.; Georgiadou, E.C.; Marin, A.; Diazmula, H.M.; Goulas, V.; Fotopoulos, V.; Tomasbarberan, F.A.; Manganaris, G.A. Metabolic and transcriptional elucidation of the carotenoid biosynthesis pathway in peel and flesh tissue of loquat fruit during on-tree development. *BMC Plant Biol.* **2017**, *17*, 102. [[CrossRef](#)] [[PubMed](#)]
36. Wang, Z.; Cui, Y.; Vainstein, A.; Chen, S.; Ma, H. Regulation of fig (*Ficus carica* L.) fruit color: Metabolomic and transcriptomic analyses of the flavonoid biosynthetic pathway. *Front. Plant Sci.* **2017**, *8*, 1990. [[CrossRef](#)] [[PubMed](#)]
37. Li, Y.; Fang, J.; Qi, X.; Lin, M.; Zhong, Y.; Sun, L.; Cui, W. Combined analysis of the fruit metabolome and transcriptome reveals candidate genes involved in flavonoid biosynthesis in *Actinidia arguta*. *Int. J. Mol. Sci.* **2018**, *19*, 1471. [[CrossRef](#)] [[PubMed](#)]
38. Paolo, B.; Saverio, O.; Mirko, M.; Matteo, B.; Lara, G.; Azeddine, S.A. Gene expression and metabolite accumulation during strawberry (*Fragaria × ananassa*) fruit development and ripening. *Planta* **2018**, *248*, 1143–1157. [[CrossRef](#)]
39. Zhang, Q.; Wang, L.; Liu, Z.; Zhao, Z.; Zhao, J.; Wang, Z.; Zhou, G.; Liu, P.; Liu, M. Transcriptome and metabolome profiling unveil the mechanisms of *Ziziphus jujuba* Mill. peel coloration. *Food Chem.* **2020**, *312*, 125903. [[CrossRef](#)]
40. Holt, R.R.; Lazarus, S.A.; Sullards, M.C.; Zhu, Q.Y.; Schramm, D.D.; Hammerstone, J.F.; Fraga, C.G.; Schmitz, H.H.; Keen, C.L. Procyanidin dimer B2 [epicatechin-(4β-8)-epicatechin] in human plasma after the consumption of a flavanol-rich cocoa. *Am. J. Clin. Nutr.* **2002**, *76*, 798–804. [[CrossRef](#)]
41. Wu, S.; Dastmalchi, K.; Long, C.; Kennelly, E.J. Metabolite profiling of Jaboticaba (*Myrciaria cauliflora*) and other dark-colored fruit juices. *J. Agric. Food Chem.* **2012**, *60*, 7513–7525. [[CrossRef](#)]
42. Boss, P.K.; Davies, C.H.J.; Robinson, S.P. Analysis of the expression of anthocyanin pathway genes in developing *Vitis vinifera* L. cv Shiraz Grape Berries and the implications for pathway regulation. *Plant Physiol.* **1996**, *111*, 1059–1066. [[CrossRef](#)]
43. Ferreyra, M.L.F.; Rius, S.P.; Casati, P. Flavonoids: Biosynthesis, biological functions and biotechnological applications. *Front. Plant Sci.* **2012**, *3*, 222. [[CrossRef](#)]
44. Pelletier, M.K.; Murrell, J.R.; Shirley, B.W. Characterization of flavonol synthase and leucoanthocyanidin dioxygenase genes in arabidopsis (further evidence for differential regulation of “early” and “late” genes). *Plant Physiol.* **1997**, *113*, 1437–1445. [[CrossRef](#)] [[PubMed](#)]
45. Dick, C.A.; Buenrostro, J.D.; Butler, T.; Carlson, M.L.; Kliebenstein, D.J.; Whittall, J.B. Arctic mustard flower color polymorphism controlled by petal-specific downregulation at the threshold of the anthocyanin biosynthetic pathway. *PLoS ONE* **2011**, *6*, e18230. [[CrossRef](#)] [[PubMed](#)]
46. Saito, K.; Yonekurasakakibara, K.; Nakabayashi, R.; Higashi, Y.; Yamazaki, M.; Tohge, T.; Fernie, A.R. The flavonoid biosynthetic pathway in Arabidopsis: Structural and genetic diversity. *Plant Physiol. Biochem.* **2013**, *72*, 21–34. [[CrossRef](#)] [[PubMed](#)]

47. Dellus, V.; Mila, I.; Scalbert, A.; Menard, C.; Michon, V.; Du Penhoat, C.L.M.H. Douglas-fir polyphenols and heartwood formation. *Phytochemistry* **1997**, *45*, 1573–1578. [[CrossRef](#)]
48. Dellus, V.; Scalbert, A.; Janin, G. Polyphenols and colour of douglas fir heartwood. *Holzforschung* **1997**, *51*, 291–295. [[CrossRef](#)]
49. Pâques, L.E.; Garciascasas, M.D.C.; Charpentier, J. Distribution of heartwood extractives in hybrid larches and in their related European and Japanese larch parents: Relationship with wood colour parameters. *Eur. J. For. Res.* **2013**, *132*, 61–69. [[CrossRef](#)]
50. Takahashi, K.; Mori, K. Relationships between blacking phenomenon and norlignans of sugi (*Cryptomeria japonica*) heartwood III: Coloration of norlignans with alkaline treatment. *J. Wood Sci.* **2006**, *52*, 134–139. [[CrossRef](#)]
51. Shao, F.; Zhang, L.; Guo, J.; Liu, X.; Ma, W.; Wilson, I.W.; Qiu, D. A comparative metabolomics analysis of the components of heartwood and sapwood in *Taxus chinensis* (Pilger) Rehd. *Sci. Rep.* **2019**, *9*, 1–8. [[CrossRef](#)]
52. Chen, S.; Yen, P.; Chang, T.; Chang, S.; Huang, S.; Yeh, T. Distribution of living ray parenchyma cells and major bioactive compounds during the heartwood formation of *Taiwania cryptomerioides* Hayata. *J. Wood Chem. Technol.* **2018**, *38*, 84–95. [[CrossRef](#)]
53. Nakaba, S.; Arakawa, I.; Morimoto, H.; Nakada, R.; Bito, N.; Imai, T.; Funada, R. Agatharesinol biosynthesis-related changes of ray parenchyma in sapwood sticks of *Cryptomeria japonica* during cell death. *Planta* **2016**, *243*, 1225–1236. [[CrossRef](#)]



© 2020 by the authors. Licensee MDPI, Basel, Switzerland. This article is an open access article distributed under the terms and conditions of the Creative Commons Attribution (CC BY) license (<http://creativecommons.org/licenses/by/4.0/>).